TISSUE ENGINEERING: Part A
Volume 16, Number 3, 2010

DOI: 10.1089/ten.tea.2009.0370

Angiogenesis in a Microvascular Construct for Transplantation Depends on the Method of Chamber Circulation

Carlos C. Chang, Ph.D.,[1] Sara S. Nunes, Ph.D.,[1] Scott C. Sibole, B.S.,[2] Laxminarayanan Krishnan, Ph.D.,[1] Stuart K. Williams, Ph.D.,[1] Jeffrey A. Weiss, Ph.D.,[2] and James B. Hoying, Ph.D.[1]

Effective tissue prevascularization depends on new vessel growth and subsequent progression of neovessels into a stable microcirculation. Isolated microvessel fragments in a collagen-based microvascular construct (MVC) spontaneously undergo angiogenesis in static conditions *in vitro* but form a new microcirculation only when implanted *in vivo*. We have designed a bioreactor, the dynamic *in vitro* perfusion (DIP) chamber, to culture MVCs *in vitro* with perfusion. By altering bioreactor circulation, microvessel fragments in the DIP chamber either maintained stable, nonsprouting, patent vessel morphologies or sprouted endothelial neovessels that extended out into the surrounding collagen matrix (i.e., angiogenesis), yielding networks of neovessels within the MVC. Neovessels formed in regions of the construct predicted by simulation models to have the steepest gradients in oxygen levels and expressed hypoxia inducible factor-1α. By altering circulation conditions in the DIP chamber, we can control, possibly by modulating hypoxic stress, prevascularizing activity *in vitro*.

Introduction

The microcirculation is a dynamic network of small-caliber blood vessels that plays an integral role in maintaining homeostasis.[1] In addition to providing nutrient delivery and metabolic waste removal, the microvasculature acts as a conduit for the local and systemic distribution of cell signals.[2] *In vivo*, microvascular beds also have the capacity to adapt to the changing needs of the surrounding tissue. In common physiological processes and in response to acute and chronic diseases, existing microvasculatures may be triggered to form new vessels (i.e., angiogenesis).[3] These neovessels extend out into the surrounding matrix, inosculating with other sprouts and newly formed microvessels. Over time, these nascent vessels become fully integrated into a microvascular network capable of providing increased perfusion tailored to the needs of the surrounding tissue.

We have developed an experimental three-dimensional system that recapitulates *in vivo* angiogenic behavior. In this microvessel fragment (MVF) model, small-caliber blood vessels (arterioles, capillaries, and venules) are isolated from rat epididymal fat and suspended within collagen matrices.[4,5] These microvessels retain their normal three-dimensional architecture and spontaneously form endothelial sprouts (i.e., angiogenesis) without the addition of exogenous angiogenic factors when cultured *in vitro*. Within 7 days, sprouts grow out into the matrix to form neovessels that inosculate with other nascent microvessels, yielding complex three-dimensional networks. *In vitro*, collagen-suspended MVFs do not progress past this angiogenic phenotype. However, if these constructs are implanted *in vivo*, construct microvessels form a new microcirculation contiguous with the host vasculature.[5] Moreover, implanted constructs develop heterogeneous vessel diameters with a hierarchical structure similar to native microvasculatures.

It is our long-term goal to parallel the *in vivo* maturation of MVF-based constructs *in vitro*. Because intravascular perfusion of constituent neovessels and nascent networks is likely critical to the progression toward a functional microcirculation within the constructs,[6–8] we have developed a bioreactor system, the dynamic *in vitro* perfusion (DIP) chamber, capable of perfusing microvascular constructs (MVCs) *in vitro*. The modular design of the DIP chamber permits a variety of different circulation configurations that, we show, significantly affect the angiogenic behavior of microvessels within *in vitro* constructs.

Materials and Methods

Microvessel fragment isolation

MVFs were isolated following previously described procedures.[4,9] Briefly, epididymal fat pads were harvested from retired Sprague-Dawley male breeder rats, minced, and

[1]Division of Cardiovascular Therapeutics, Cardiovascular Innovation Institute, Louisville, Kentucky.
[2]Department of Bioengineering, University of Utah, Salt Lake City, Utah.

digested with collagenase. MVFs were rinsed, filtered through sterile nylon screens (500 and 20 μm pore size), collected, and kept on ice until used. Sterile, acidified rat-tail collagen type I (BD Biosciences, San Jose, CA) was mixed with ice-cold water, 4×Dulbecco's modified Eagle's medium (DMEM) (Invitrogen, Carlsbad, CA), and 1 N NaOH to yield a final concentration of 3 mg/mL collagen and 1×DMEM at pH 7.4. Isolated MVFs were mixed in with the unpolymerized collagen and maintained on ice until used.

DIP chamber assembly and medium circulation

Sterile support components (nylon circumferential screen, poly[tetrafluoroethylene] support flares), and polymer mandrel (20-gauge poly[tetrafluoroethylene]; Small Parts, Miramar, FL) were aseptically placed within a central module (Figs. 1a, b). A hydrogel (Pluronic F-127; Sigma-Aldrich, St. Louis, MO; 30% by weight in divalent-cation-free phosphate-buffered saline) was applied to the bottom of the central module providing a seal to prevent collagen leakage (Fig. 1b). Three milliliters of MVF/collagen was delivered to the central module and then placed in a tissue culture incubator. After polymerization for 60 min, the top and bottom modules were added to the assembly, and the central polymer mandrel was slowly removed, forming an artificial lumen within the MVF construct. Each DIP chamber module was then connected to gas permeable tubing with an inline medium reservoir. Modules were perfused with the circulation medium (low-glucose DMEM (Invitrogen) with 10% fetal bovine serum (FBS; Gemini Bioproducts, West Sacramento, CA), 1% penicillin/streptomycin (Invitrogen), and 0.13% Fungizone (Invitrogen) with a volumetric flow rate of 1.5 mL/min (Fig. 1c). For experimental analysis, constructs were conditioned with the circulation medium via two

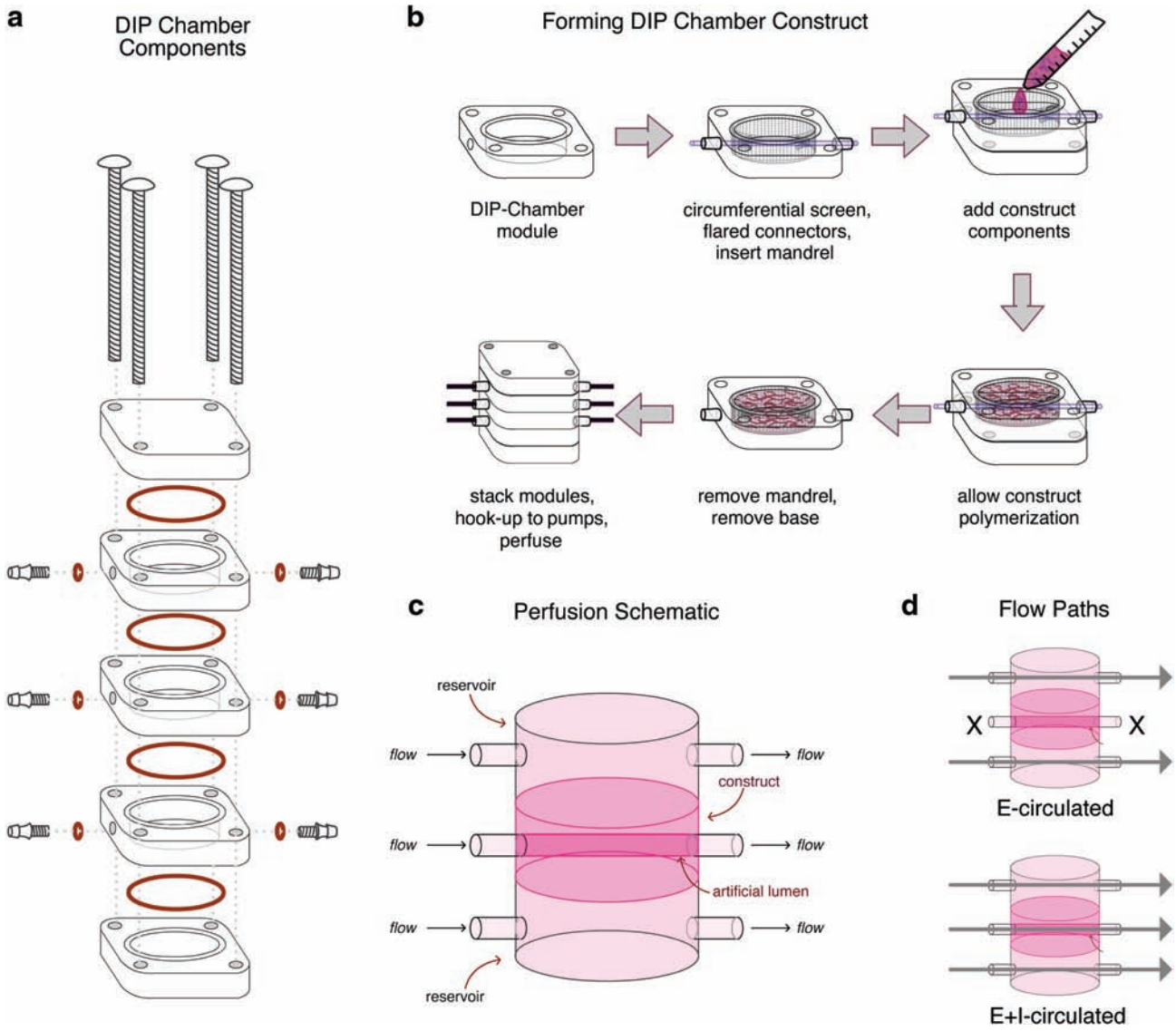

FIG. 1. Schematic of the dynamic *in vitro* perfusion (DIP) chamber. (**a**) DIP chamber components are illustrated. (**b**) Illustration of DIP chamber central module assembly. (**c**) A schematic representation of perfusion through a three-module DIP chamber is provided. (**d**) Illustrations of the two perfusion schemes utilized in the presented experiments are provided: E-circulated and E+I-circulated. Color images available online at www.liebertonline.com/ten.

methods (Fig. 1d). The medium was circulated over either external (E-circulated) or external and internal (E+I-circulated) surfaces. DIP chambers (12 total) were conditioned for 10 days: three each of E-circulated and E+I-circulated constructs for fluorescent microscopy, three each of E-circulated and E+I-circulated constructs for paraffin sectioning.

Histology and immunohistochemistry

E- and E+I-circulated DIP chamber constructs were prepared for paraffin sectioning and hematoxylin and eosin and *Griffonia simplicifolia-1* (GS1) as previously described.[10] Hypoxia inducible factor-1α (HIF1α) staining paralleled the GS1 protocol substituting the lectin for a biotintylated-anti-HIF1α antibody (Novus Biologicals, Littleton, CO). DIP chamber–conditioned constructs were sectioned perpendicular to the artificial lumen.

Microvessel density analysis

GS1-positive vessels were counted on each slide (Fig. 2). The cross-sectional area of each analyzed slide section was determined by first capturing digital images of each section. These images were then assembled in Adobe Photoshop. The area of each section was manually traced and then calculated with the Area Calculator plug-in for ImageJ (http://rsbweb.nih.gov/ij/). Vessel counts, lumen counts, and area calculation were repeated for three sections of each sample.

Viability analysis

Construct viability was determined via fluorescent image analysis by a custom Matlab program (Mathworks, Natick, MA). Samples were first cut in half, perpendicular to the central lumen. Constructs were then assayed with Live/Dead Viability/Cytotoxicity Kit for 1 h. Samples were placed on a glass slide, with the cut surface toward the objective. Evaluations were divided into three regions of interest (ROI) (Fig. 3a). ROI1 included an ~2-mm-thick region of the construct immediately adjacent to the central artificial lumen (represented with an L), ROI3 included an ~2-mm-thick region of the construct immediately adjacent to the external surface of the construct, and ROI2 included the region between ROI1 and ROI3 (~2 mm thick). Image pairs comprised of a viable image (positive calcein AM staining) and a nonviable image (positive ethidium homodimer-1) of the same field of view were processed. The analysis used previously described automated thresholding and size-filtering methods, maintaining the integrity of microvascular structures.[11] Fragment viability was expressed as a ratio of the live vessel count to the total structures obtained by overlaying the thresholded and size-selected structures within paired images. This ratio was expressed as a percentage and compared across groups. Five image pairs from each ROI from each sample were analyzed.

Sprouting analysis

A scoring system was used to evaluate the sprouting characteristics of microvessel constructs and DIP chamber–conditioned E- and E+I-circulated constructs (for example scores, see Supplemental Material, available online at www.liebertonline.com/ten). A score of 0 represented no visible MVF sprouting. A score of 1 represented fragments with a few small, scattered sprouts, while a score of 2 represented a construct with extensive sprouting, many of significant length. Three independent observers viewed randomized fluorescent images and scored each image individually. The scores were compiled and analyzed.

HIF1α en bloc *immunostaining*

Control and hypoxic day 5 constructs were immunostained as previously described.[9] Biotintylated-anti-HIF1α was used to investigate MVF HIF1α production. Immunostained samples were imaged with an Olympus FV1000 MPE Confocal System. Image stacks were captured with identical laser and detector settings and volume rendered in Amira 5.2 (Visage Imaging, San Diego, CA).

Hypoxia and vascular endothelial growth factor inhibition experiments

Two separate MVF isolations were pooled to prepare the MVF constructs for the hypoxia experiments. About 250 μL of MVF–collagen suspension was dispensed into individual wells of a 48-well plate and allowed to polymerize for 15 min. After adding 250 μL of 1×DMEM with 10% FBS, constructs were placed in a standard tissue culture incubator (5% CO_2 and 37°C). For hypoxia studies, samples were maintained within an airtight chamber with inlet and outlet ports connected to a pressurized cylinder containing 1% O_2, 7% CO_2, and 92% N_2. After flushing for 10 min the two ports were sealed, the containers were placed within a tissue culture incubator and cultured. A total of eight samples (four hypoxic and four control) were collected and daily assayed for viability for 7 days. After removing samples from the hypoxic well plates, the opened chamber was immediately resealed and the chamber was flushed again as described above. All constructs were assayed with the Live/Dead Viability/Cytotoxicity Kit (Invitrogen) for 1 h, rinsed with divalent-cation-free phosphate-buffered saline, and fixed with 2% paraformaldehyde.

Alternatively, for vascular endothelial growth factor (VEGF) inhibition studies, constructs received DMEM+10% FBS supplemented with or without (control) either a cocktail of soluble recombinant VEGFR1/R2 Fc chimeras, Fc control (57 μM; R&D, Minneapolis, MN), or a small inhibitor of VEGF signaling (Cyclo-VEGI, 50 μM; Calbiochem, San Diego, CA[12]). Images were captured after 7–10 days in culture, captured with an Olympus IX71 inverted microscope fitted with an Olympus DP71 digital camera.

DIP chamber computational model

The DIP chamber construct geometry was discretized into a hexahedral finite element (FE) mesh with 25,920 elements using TrueGrid (XYZ Scientific, Livermore, CA) software. A mesh convergence study was used to determine this optimal mesh density. The mesh was imported into the ABAQUS FE framework and assigned a transient mass diffusion constitutive model (Supplemental Material). This constitutive model required two parameters: mass concentration and the diffusion coefficient. The medium oxygen concentration was prescribed to be the partial pressure for oxygen in water (3.712×10^{-8} g/mm^3). The initial concentration of oxygen in

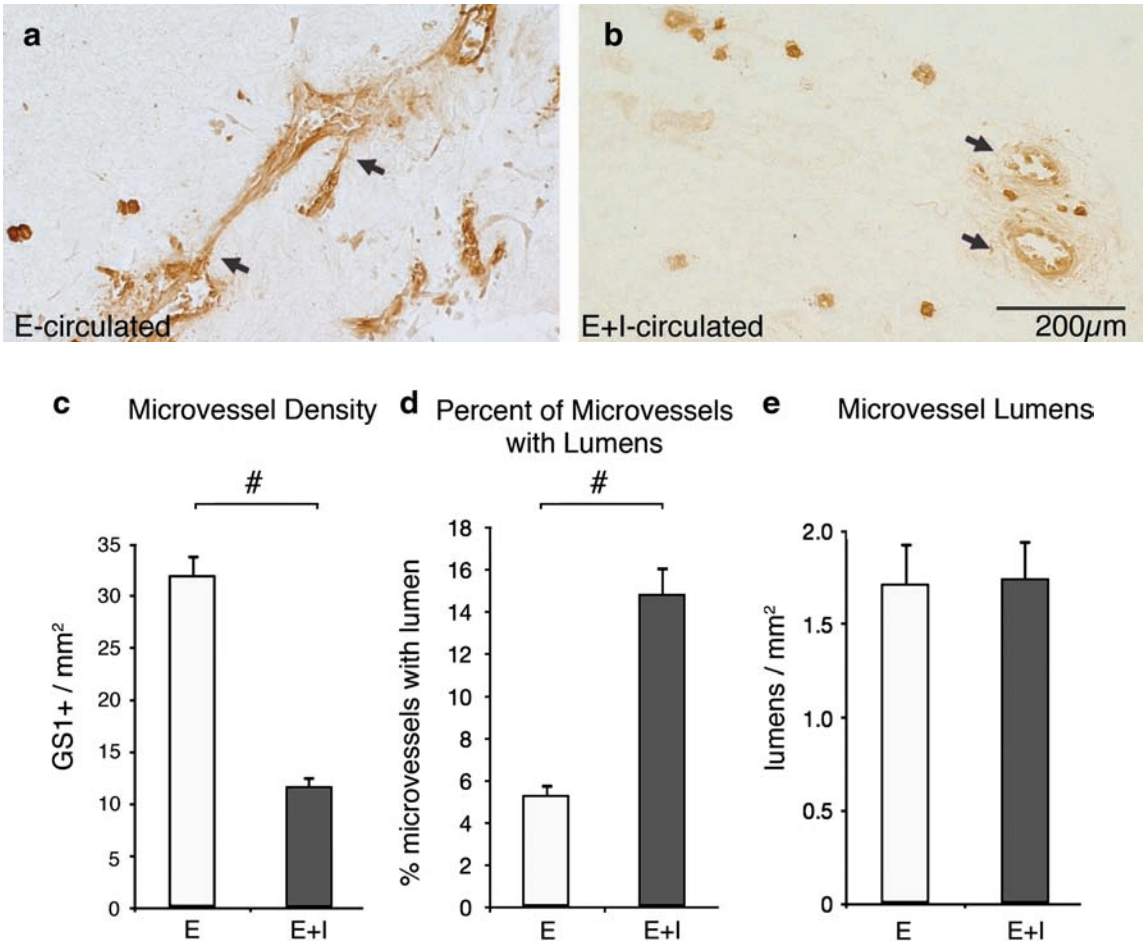

FIG. 2. Vessel density in DIP chamber constructs. (**a**) In E-circulated constructs, endothelial (brown) sprouts appear to extend out into the matrix and, in some instances, inosculate other vessels (arrows). Within E+I-circulated constructs (**b**), many patent microvessels were found, but little sprouting was evident (arrows). E-circulated constructs contained significantly more microvessels (**c**) and fewer patent microvessels (**d**) than E+I-circulated sections ($^{\#}p < 0.0001$). (**e**) If lumen number was normalized to construct cross section, there was no significant difference between E-circulated and E+I-circulated samples ($p = 0.93$). All calculated values are presented as mean ± standard error of the mean (s.e.m). The scale bar for (**a**) and (**b**) is 200 μm. Color images available online at www.liebertonline.com/ten.

the collagen was assumed to be zero based on worst-case simulations of oxygen equilibrium between collagen and air using Henry's law. The diffusion coefficient of oxygen in collagen was calculated to be $D_{O2} = 2.286 \times 10^{-3}$ mm^2/s (Supplemental Material). Due to the low volume ratio of microvessels to collagen and the relatively low metabolic rate of vascular cells, estimated oxygen consumption (see Supplemental Material) was assumed to be negligible. The flow rate through the circulation ports was low enough to ignore effects of turbulence and advection. The oxygen concentration on the surface of the tube that delivered the medium to the culture was assumed to be constant based on the Peclet number (see Supplemental Material). Longitudinal and axial cross-sections were provided for simulations at 6, 12, and 18 h, allowing internal comparisons of oxygen diffusion.

Statistical analysis

Statistical analysis was conducted with JMP 7.0.1 (SAS, Cary, NC). Analysis of variance (ANOVA) and two-tailed Student's *t*-test analyses were used to compare continuous data. Pearson's chi-square analysis was used to assess ordinal and nominal data. The calculated *p*-values were presented where applicable, unless values were smaller than 0.0001. Tests were considered significant if the *p*-value was less than or equal to 0.05. To further analyze the relative significance of group differences within ANOVA analysis, the Tukey honestly significant difference (HSD) least square means differences analysis was used. This method of multiple comparisons uses stringent comparison structures to conservatively calculate statistical significance.[13] All tests performed by Tukey HSD analysis were conducted with $\alpha = 0.050$. All calculated values are presented as mean ± standard error of the mean.

Results

DIP chamber

The DIP chamber was designed as a reconfigurable, multimodule system for supporting the culture of soft tissues (Fig. 1a). It consists of three perfused modules with internal

cylindrical volumes of approximately 3 mL (inner diameter of 17.5 mm and height of 12.5 mm). In the employed configuration, MVCs were formed around a mandrel within the center module of a three-module stack (Fig. 1b). This mandrel was later removed, forming a central lumen that was contiguous with external circulation ports. Within the chamber, a passive biocompatible frame maintained the construct position and shape during culture (see Materials and Methods section). Once the DIP chamber with an MVC was assembled, the medium was circulated over the outer surfaces and through the construct via the central lumen (Fig. 1c). Depending on module configurations, circulation through the chamber can occur via a number of pathways.

Our earlier work with MVCs typically involved MVF seeding densities of 15,000 to 20,000 MVFs per mL of collagen.[4,5] Once formed into constructs of 100 to 500 μL volumes, these constructs were cultured in well plates under static conditions (the constructs were not exposed to medium circulation) in which the culture medium was replaced every 4 days.[4,5,9] As previously described, the MVFs undergo spontaneous sprouting and neovessel growth.[4,5,9] In standard conditions (DMEM+10% FBS), microvessel density is 62 (±2.1) microvessels per μm^2 with approximately 90% (±1.3%) MVF viability after 6 days of culture. In an attempt to recreate the conditions of these static cultures in the DIP chambers, we evaluated two different chamber-conditioning protocols (Fig. 1d). The first involved the circulation of the medium through all three modules (E+I-circulated) and represents, for the DIP chamber configuration, full nutrient delivery. The second involved circulating through only the top and bottom modules (E-circulated), which represents partial delivery of nutrients. We attempted alternate circulation protocols including trans-module circulation schemes (i.e., perfusing into the bottom module, through the center chamber, and out the top module). However, the resistance to medium flow through the collagen construct in this configuration was too large; the subsequent pressure differential displaced the construct from the central module.

Culture of microvessels in the DIP chamber

All constructs were formed with similar initial MVF densities, approximately 20,000 MVFs per mL. However, after 10 days of DIP chamber culture, there were clear differences in MVF phenotype between the constructs conditioned by the two different circulating protocols (Fig. 2). Microvessel density (GS1-positive structures/area) in the E-circulated condition was more than twice as high as that for the E+I-condition (Fig. 2c). In contrast, the relationship between the fractions of microvessels with clearly patent lumens in the E-circulated condition was opposite to that observed for densities (Fig. 2d). In the E+I-circulated constructs, nearly three times as many microvessels exhibited a clearly patent lumen compared with microvessels in the E-circulated cultures. Interestingly, constructs cultured with both circulation conditions had similar numbers of lumen-containing structures per area. When we assume that the microvessels with patent lumen likely represent parent MVFs, this suggests that relatively similar numbers of parent MVFs persisted in the constructs from the initial seeding density.

The similar number of lumens in E- and E+I-circulated constructs also suggests the additional microvessels present in the former may be due to nonpatent new vessel growth. To address this, we evaluated the relative extent of neovessel sprouting and growth in the two culture conditions (Table 1; Supplemental Material). As predicted, the extent of sprouting was considerably greater in the E-circulated cultures than in the E+I-circulated cultures (Fig. 3b). Unlike the E+I-circulated condition, where sprouting was uniformly minimal throughout the construct, E-circulated conditioned constructs contained regional differences in the extent of sprouting (Fig. 3b). The differences in sprouting index did not correlate with microvessel viability (Fig. 3c). Despite small yet significant differences in viability between different regions of the constructs (ANOVA, $n = 45$, F-ratio $= 3.72$, $p = 0.0325$), overall microvessel viability between the two different conditions was not substantially different (two-tailed Student's t-test, $n = 90$, df $= 83.95$, $p = 0.6203$).

Modeling oxygen diffusion within DIP chamber constructs

The difference in the angiogenic response in the DIP chamber suggests that concentrations of essential factors within the constructs were different in the E- and E+I-circulated protocols. Focusing on the differences in sprouting between the two conditions, we first hypothesized that a decrease in oxygen availability within E-circulated constructs leads to increased angiogenic sprouting. To begin testing this hypothesis, we performed an analysis of oxygen mass transport in a DIP chamber by designing a FE computer model that incorporated the unique geometry of the construct (Fig. 4a). In the simulation, initial oxygen concentration within the construct was assumed to be zero, and oxygen consumption during culturing was considered negligible. According to the computational model, oxygen levels within the DIP chamber constructs equilibrated to those in the medium (assumed 21%) within 48 h regardless of the circulation scheme (Fig. 4b). However, it took approximately 1.3 h longer to reach 50% equilibrium and 2.8 h longer for 75% equilibrium in E-circulated constructs. Further, results of the simulations suggest that oxygen gradients formed and persisted longer within the region in which sprouting was most prevalent (in the E-circulated constructs) (Fig. 4c, d). Additionally, the region nearest the central lumen remained hypoxic for the longest period of time.

Angiogenesis in the MVCs is oxygen sensitive

Based on the simulations, we hypothesized that the difference in sprouting angiogenesis between the E- and E+I-circulated constructs may be due to some degree of hypoxic insult. To investigate the effects of oxygen concentration on microvessel behavior, we compared DIP chamber–conditioned constructs to standard MVCs[4,5] cultured in hypoxic and normoxic conditions. E- and E+I-circulated constructs were assayed for the presence of the hypoxia marker HIF1α.[14] Microvessels, including neovessels, present only in the E-circulated constructs stained positively for HIF1α (Fig. 5a–d). Positive HIF1α immunostaining was particularly prevalent in the outer region of the construct in the E-circulated cultures, which is the zone exhibiting the highest index of sprouting (ROI3 in Fig. 3). To further investigate the effects of hypoxia on MVF angiogenesis, MVCs were cultured under static conditions and exposed to standard (21% O_2) or

Table 1. Summary of DIP Chamber Results

	Vessel density microvessel/mm²	*% Microvessel with lumen*	*Lumen per mm²*	*Sprouting (sprouting index)*			*Viability (% viable)*			*HIF1α*	*75% [O₂] (hours)*
				ROI1	*ROI2*	*ROI3*	*ROI1*	*ROI2*	*ROI3*		
E-circulated	32.0 ± 2.0^{a}	5.3 ± 0.6^{a}	1.71 ± 0.22^{i}	0.6 ± 0.06^{b}	0.8 ± 0.09^{b}	1.4 ± 0.08^{b}	$69 \pm 5.1^{c,g}$	$76 \pm 3.4^{d,g}$	$57 \pm 5.9^{c,d,g}$	+	14.4
E+l-circulated	11.7 ± 1.1^{a}	14.8 ± 1.3^{a}	1.74 ± 0.21^{i}	0.16 ± 0.05	0.18 ± 0.06	0.24 ± 0.06	$85 \pm 3.6^{e,f,h}$	$58 \pm 6.3^{e,h}$	$52 \pm 6.1^{f,h}$	−	11.6
	$^{a}p < 0.0001$	$^{a}p < 0.0001$	$^{i}p = 0.93$		$^{b}p < 0.0001$		$^{g}p = 0.325$	$^{c-f}\alpha = 0.05$	$^{h}p = 0.0002$		

Superscripts within summary table denote statistical significance of compared values. a: $p < 0.0001$, b: $p < 0.0001$, c: $\alpha = 0.05$, d: $\alpha = 0.05$, e: $\alpha = 0.05$, f: $\alpha = 0.05$, g: $p = 0.325$, h: $p = 0.0002$, i: $p = 0.93$.

hypoxic (1% O_2) conditions (representing the worst-case scenario within the E-circulated constructs). Microvessels in both conditions stained positive for HIF1α (Fig. 5e–f), suggesting that even microvessels under the standard, assumed normoxic (i.e., 21% oxygen) conditions were experiencing hypoxic stress. As expected,[4,5,9] MVFs cultured under standard conditions exhibited considerable sprouting and neovessel growth (Fig. 5i). In contrast, MVFs cultured in 1% oxygen conditions sprouted very little or not at all and no neovessel growth was observed (Fig. 5i). Additionally, MVFs cultured under hypoxic conditions exhibited reduced viability, but only later in the culture period (Fig. 5j). This delayed viability decrease suggests that the level of hypoxia in the 1% oxygen conditions was too detrimental to MVF health and integrity for angiogenesis to occur. Given that sprouting occurred from and HIF1α was expressed in microvessels of standard, static MVCs and the E-circulated constructs in the DIP chamber, it seems likely that the level of hypoxic stress was similar in both culture conditions.

Microvessel sprouting in cultures does not depend on VEGF

The expression of HIF1α by MVFs in the static and E-circulated constructs suggested that downstream autocrine VEGF may explain the accompanying angiogenesis within the MVC.[14–16] Therefore, to assess the role of two common isoforms of VEGF (VEGF-A and VEGF-B), we included either a cocktail of soluble VEGFR1 and R2[17] or a small molecule inhibitor of VEGF signaling, Cyclo-VEGI[12]), in the culture medium of standard, static MVC cultures. Neither the soluble VEGFR1/R2 cocktail (Fig. 6b, c) nor the Cyclo-VEGI (Fig. 6d, e) prevented MVF sprouting in static constructs, suggesting that microvessel sprouting was independent of VEGF. This was corroborated by the lack of VEGFR2 activation (phosphorylation) in the samples by Western blotting (data not shown) and is in accordance with the lack of change in mRNA levels for both VEGF and VEGFR in the static cultures throughout the culture period.[18]

Discussion

The DIP chamber was developed to provide a means to circulate medium around and through a prevascularized tissue construct. While designing the DIP chamber, we incorporated features to support four objectives: (1) provide flexibility in bioreactor utility, (2) support the shape and integrity of soft tissue constructs, (3) support microvessel viability and neovascular growth, and (4) provide a potential avenue for intravascular perfusion of the neovascular network. The modular character of the DIP chamber provided flexibility in its use by combining any number of stacked modules. In the described configuration, we selected a three-module bioreactor with each module accommodating direct circulation. A module either circulated medium (i.e., the top and bottom modules) or supported an MVC (the central module). Since we use soft, collagen-based constructs, we developed biocompatible internal supports to maintain the size and position of the MVC within the module. The supports were also designed to permit collagen polymerization around a removable mandrel. This mandrel, once removed, formed an artificial lumen within the construct that was contiguous with the inflow and outflow ports of the surrounding mod-

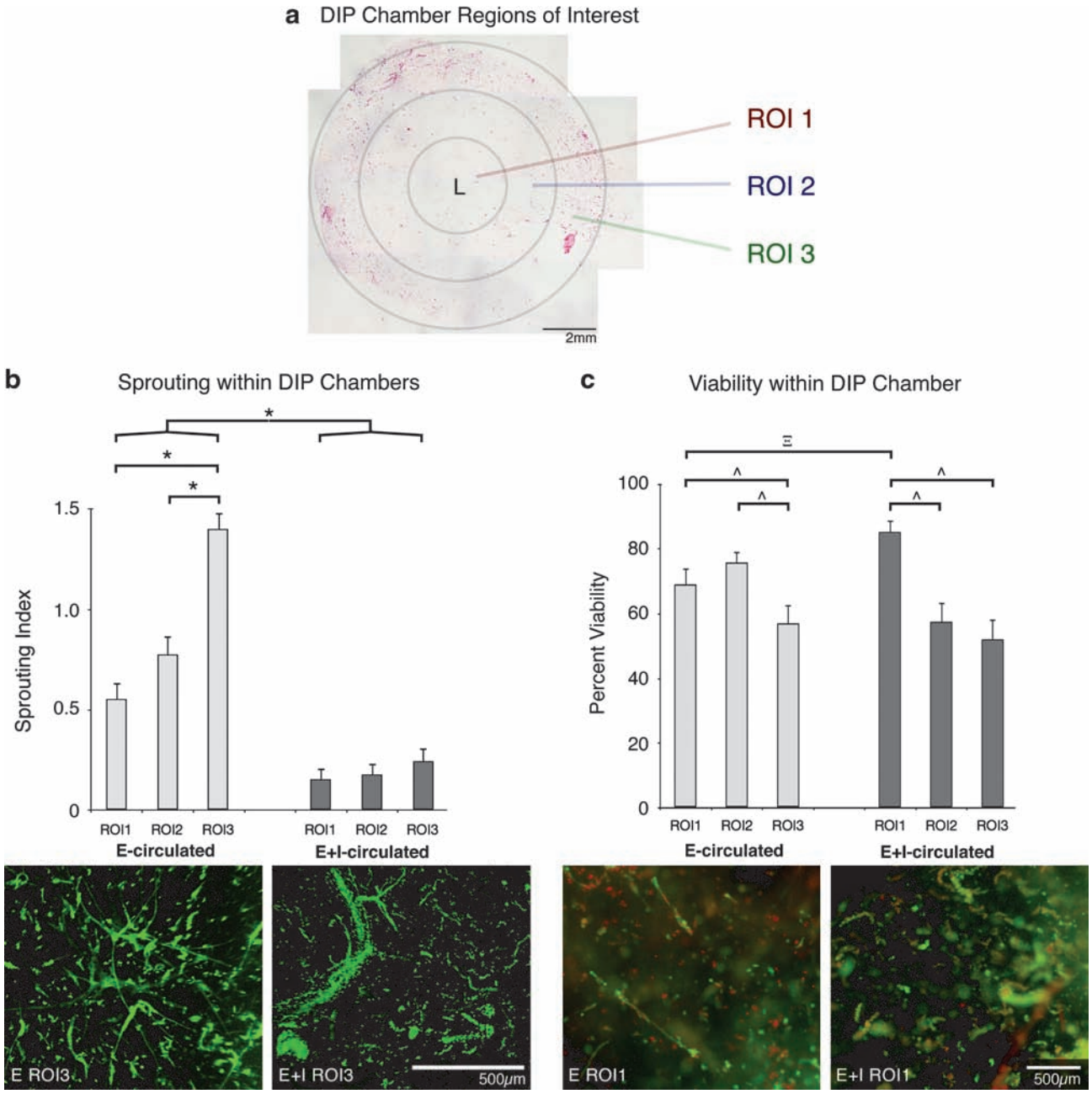

FIG. 3. Microvessel characterization within DIP chamber constructs. (**a**) Investigation of DIP chamber constructs focused on three regions of interest (ROI) surrounding the central lumen (L). An example E-circulated construct cross section is presented for illustration. (**b**) When microvessel sprouting was assessed, E-circulated constructs averaged more sprouting fragments than E+I-circulated constructs ($^{*}p < 0.0001$). In the E-circulated condition, angiogenesis was highest at the periphery of the construct and lowest in the region nearest to the noncirculated central lumen. Example ROI3 images of E- and E+I-circulated constructs are provided. Green represents viable microvessel fragments (MVFs). (**c**) There was no significant difference between E- and E+I-circulated fragment viability ($p = 0.6203$). However, there was a significant difference among E-and E+I-circulated ROIs ($\hat{}\alpha = 0.05$). In addition, the viability of fragments within E-circulated ROI1 was significantly less than E+I-circulated ROI1 counterparts (two-tailed Student's t-test, $n = 30$, $\mathrm{df} = 25.05$, $^{\Xi}p = 0.0158$). Example viability images are provided for E- and E+I-circulated ROI1. Green represents viable fragments; red represents nonviable fragments. Yellow fragments contain both viable and nonviable cells. The scale bar represents 500 μm for both images. All calculated values are presented as mean ± s.e.m.

ule, thereby providing a central conduit for potential intravascular perfusion.

In the DIP chamber, medium circulation through the central lumen substantially impacted the development of a neovascular network via angiogenesis; microvessel density, microvessel distribution throughout the construct, and angiogenic activity were all influenced by the method of chamber circulation. Surprisingly, the E-circulation scheme, which presumably provides submaximal medium delivery, was clearly the most effective at promoting angiogenesis and construct

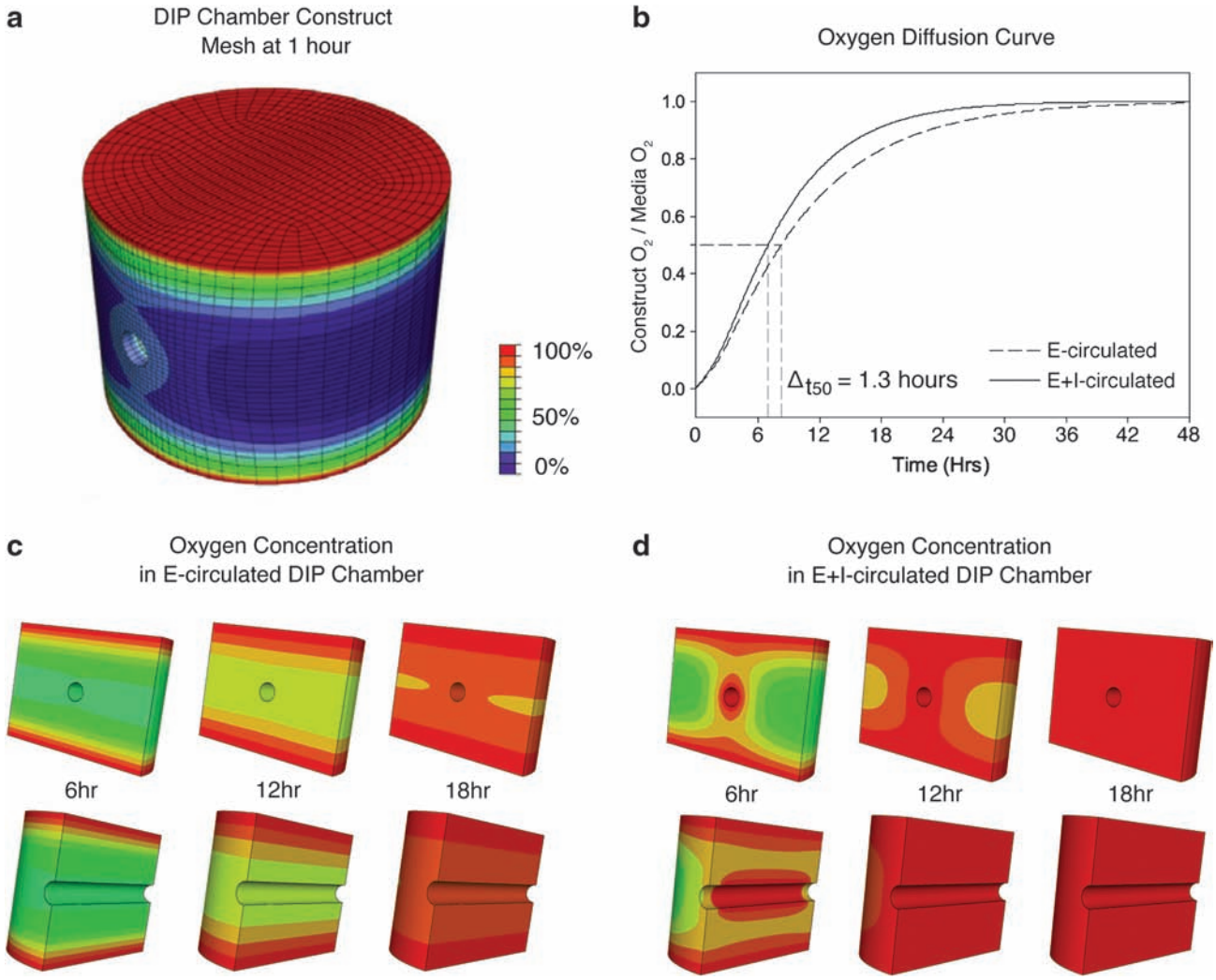

FIG. 4. Modeling oxygen transport within DIP chamber constructs. (**a**) The DIP chamber construct geometry was discretized into a hexahedral finite element mesh with 25,920 elements that had converged to a stable solution. (**b**) When we assume an oxygen molecule hydrodynamic radius of 159×10^{-9} mm, diffusion coefficient $D_{O2}=2.286\times10^{-3}$ mm^2/s (Supplemental Material), and an initial oxygen concentration of zero, E- and E+I-circulated constructs equilibrate to medium oxygen levels in approximately 48 h. Both axial and longitudinal cross sections are presented for selected time points in E-circulated (**c**) and E+I-circulated (**d**) models. According to the model, perfusion through the central port of E+I-circulated constructs increased the rate of oxygen diffusion into the construct volume. After 18 h of perfusion, nearly 91% of the E+I-circulated construct is equilibrated to medium O_2 concentration compared to 83% of the E-circulated volume.

prevascularization. Constructs supported by E-circulated conditions exhibited significantly greater microvessel density and neovessel sprouting. Microvessels in the E+I-circulated DIP chambers maintained lumen structure and viability but exhibited no angiogenic sprouting. The differences between the two circulation protocols suggest that the potential shortcomings in culture conditions, assumed to be present in the E-circulated protocol, are important in inducing angiogenesis from intact vessel elements (or a preexisting microvessel network) *in vitro*. Conversely, conditions that are perhaps more ideal in supporting tissue health, such as those presumed to be present in the E+I-circulated scheme, may act to stabilize and mature microvessels. In addition to the implications on the relationship between microvessel stability and angiogenesis, these particular findings suggest that it may be possible to control angiogenesis in tissue constructs simply by modulating the level of stress to the system. When angiogenesis is desired, the system would be stressed (by reducing medium flow to the bioreactor in our case), while reestablishing high levels of chamber circulation may act to return the system to a stable situation (i.e., mature the forming neovessels).

The reduced medium delivery in the E-circulated condition could result in limited delivery of a nutrient (i.e., oxygen) or factor important in maintaining microvessel stability and/or accumulation of a destabilizing factor (i.e., angiogenic factor). Even though we did not measure discrete oxygen concentrations in DIP chamber constructs, the increased expression of HIF1α, a protein synthesized in response to hypoxia,[19] in microvessels (both parent microvessels and neovessels) in E-circulated chambers strongly argues for a condition of reduced oxygen levels in these cultures. Given the known role of hypoxia in causing microvessel instability

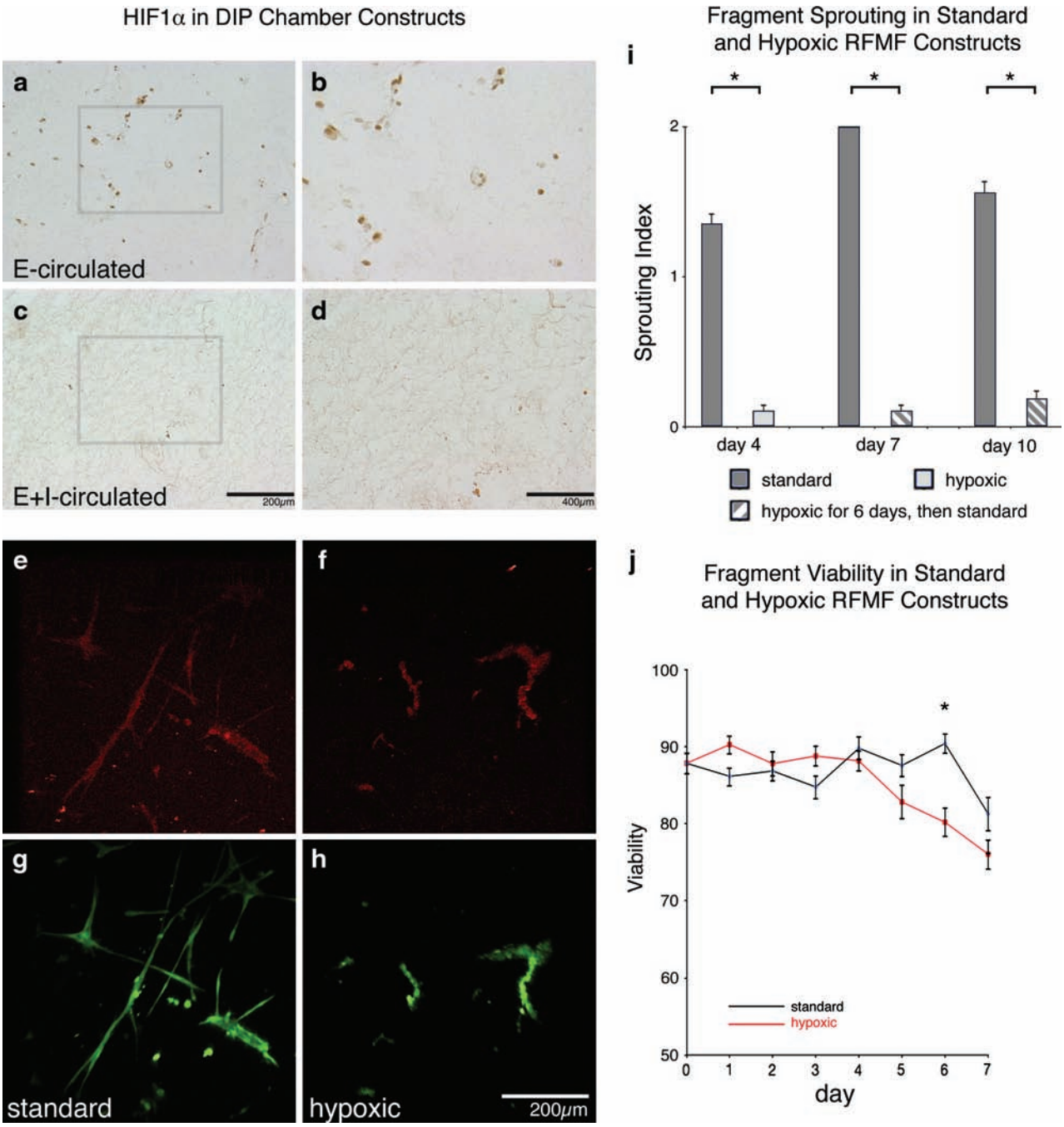

FIG. 5. Fragment viability, and sprouting in hypoxic conditions. E- and E+I-circulated DIP chamber–conditioned constructs were sectioned and stained for HIF1α (brown indicates positive staining). HIF1α-positive fragments were found throughout E-circulated constructs, but where highly concentrated in ROI3 (**a** and **b**). In E+I-circulated constructs, few HIF1α fragments were present within examined sections. Example E+I-circulated ROI3 images are presented (**c, d**). Gray boxes in (**a**) and (**c**) illustrate magnified fields of view in (**b**) and (**d**). About 250 μL MVF constructs were cultured in standard (typical cell culture conditions, 5% CO_2 and 37°C) and hypoxic conditions (1% O_2 and 37°C). Day 5 standard and hypoxic constructs were stained with a fluorescently labeled anti-HIF1α followed by three-dimensional stack generation via confocal microscopy. Stained standard constructs (**e**) presented less fluorescent signal than hypoxic constructs (**f**). MVFs were costained with a viability marker (green represents viable fragments **[g, h]**). Three time-points were selected for evaluating sprouting within cultured constructs (**i**). After 4 days of hypoxic conditioning, standard constructs (average sprouting index [ASI] of 1.35 ± 0.07) displayed significantly more sprouting than hypoxic constructs (ASI of 0.1 ± 0.04) (Pearson Chi-square test, $n = 96$, df = 2, $\chi^2 = 78.78$, $^*p < 0.0001$). After 7 days, standard constructs exhibited more sprouting than previously hypoxic constructs, respectively, ASI of 2.0 ± 0 and 0.1 ± 0.04 (Pearson Chi-square test, $n = 96$, df = 2, $\chi^2 = 96.0$, $^*p < 0.0001$). Similarly, day 10 standard samples (ASI of 1.56 ± 0.08) exhibited more sprouting than previously hypoxic specimens (ASI of 0.19 ± 0.06) (Pearson Chi-square test, $n = 96$, df = 2, $\chi^2 = 67.67$, $^*p < 0.0001$). After 6 days of culture (**j**), MVF viability was significantly less in hypoxic constructs than standard constructs, $80 \pm 2.0\%$ and $90 \pm 1.3\%$ respectively (two-tailed Student's *t*-test, $n = 40$, df = 37.54, $^*p < 0.0001$). Hypoxic cultures were then returned to standard conditions, but viability did not significantly change after 1 day of standard culturing. All calculated values are presented as mean ± s.e.m. HIF1α, hypoxia inducible factor-1α. Color images available online at www.liebertonline.com/ten.

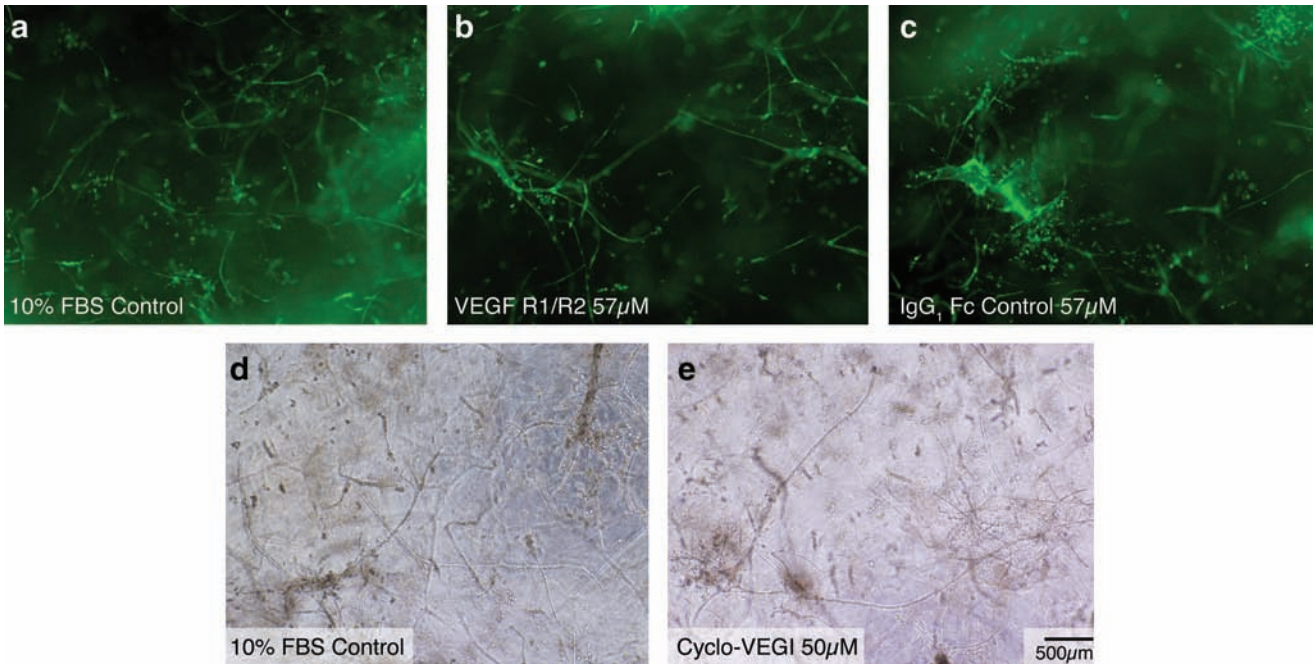

FIG. 6. Microvessel sprouting in the presence of soluble VEGF R1/R2 and VEGF inhibitor. (**a**) In control conditions, collagen-suspended microvessels form extensive networks of neovessels within 10 days. To investigate the effect of VEGF within these static cultures, soluble VEGF receptor 1 and VEGF receptor 2 (R1/R2) were added to the construct medium at a concentration of 57 μM (**b**). As a control experiment, recombinant IgG_1 Fc antibody was added to the construct medium at an equimolar concentration of 57 μM (**c**). To further investigate the role of VEGF within our microvascular constructs, Cyclo-VEGI, a small molecule inhibitor of VEGF, was added to the construct medium at a 50 μM concentration (**e**). Neither soluble VEGF R1/R2 nor Cyclo-VEGI prevented microvessel angiogenesis *in vitro*. In images (**a–c**), fragments were stained with *Griffonia simplicifolia*-1 (green), a marker for endothelial cells. Images (**d**) and (**e**) are brightfield images. The scale bar for all images is 500 μm. VEGF, vascular endothelial growth factor; FBS, fetal bovine serum. Color images available online at www.liebertonline.com/ten.

and promoting angiogenesis,[20,21] it seems very likely that hypoxia is contributing to angiogenesis in the E-circulated DIP chambers. However, we cannot rule out the possibility that an important factor for angiogenesis accumulates in the E-circulated condition but is washed out in the E+I-circulated condition. If oxygen delivery is important, it is not yet clear as to the range of oxygen tensions necessary for promoting angiogenesis in the constructs; clearly, extreme hypoxia (i.e., 1% O_2), as was present in the static MVC cultures, negatively affects microvessel sprouting.

Increased production of HIF1α has also been correlated to increased production of VEGF in endothelial and other cell types.[15] Therefore, it seemed likely that the increased expression of HIF1α in the constructs would lead to increased autocrine VEGF production, which would then lead to angiogenic sprouting. However, blockage of VEGF signaling via two different inhibitors did not cause a profound decrease in angiogenesis in MVCs. Therefore, it is unlikely that VEGF is responsible for the angiogenic sprouting observed in the E-circulated cultures. Whether or not VEGF is influencing neovessel phenotypes in a way other than neovessel growth (e.g., changing diameters) is unclear. HIF1α is known to regulate the expression of a number of factors relevant to angiogenesis,[14] which could very possibly be an important stimulus for neovessel sprouting and growth in our microvessel system.

We have not yet systematically examined if any of the neovessels in the constructs cultured in the DIP chamber, particularly in the E-circulated condition, are perfusion competent. Ultimately, we intend to assemble a new microcirculation within the DIP chambers capable of transporting, intravascularly, a circulating medium. From our data, it would appear that the parent MVFs maintained a patent lumen (in both the E- and E+I-circulated conditions), whereas the neovessels that sprouted from the MVFs in the E-circulated conditions did not. However, the absence of a clear lumen in the new sprouts and neovessels may reflect the absence of hemodynamic conditioning thought important in post-angiogenesis maturation and neovessel stability.[7,8] Therefore, it may be necessary to initiate intravascular perfusion, perhaps via a strategy involving the central circulation port and a potential connection to the neovascular network, to cause the neovascular network that does form in the DIP chamber to progress toward a mature microvessel network complete with contiguous lumen. However, such a strategy would have to take into account the antiangiogenic conditions created by perfusing the chamber through the central port (i.e., E+I-circulated protocol). However, if sprouting angiogenesis in the DIP chamber constructs reflects a specific oxygen tension, then perhaps it is possible, by culturing under defined partial pressures of oxygen in the incubator, to manipulate angiogenesis in constructs, not by altering medium delivery but by changing starting oxygen levels. With such modifications, it may be possible to form, *in vitro*, functional microvascular networks.

Disclosure Statement

There are no conflicting commercial associations or financial interests to disclose for any author.

References

1. Tortora, G.J., and Grabowski, S.R. Principles of Anatomy and Physiology. 10th edition. New York: John Wiley & Sons, 2003.
2. Secomb, T.W., and Pries, A.R. Information transfer in microvascular networks. Microcirculation **9,** 377, 2002.
3. Folkman, J. Angiogenesis: an organizing principle for drug discovery? Nat Rev Drug Discov **6,** 273, 2007.
4. Hoying, J.B., Boswell, C.A., and Williams, S.K. Angiogenic potential of microvessel fragments established in three-dimensional collagen gels. In Vitro Cell Dev Biol Anim **32,** 409, 1996.
5. Shepherd, B.R., Chen, H.Y., Smith, C.M., Gruionu, G., Williams, S.K., and Hoying, J.B. Rapid perfusion and network remodeling in a microvascular construct after implantation. Arterioscler Thromb Vasc Biol **24,** 898, 2004.
6. Frerich, B., Zueckmantel, K., and Hemprich, A. Microvascular engineering in perfusion culture: immunohistochemistry and CLSM findings. Head Face Med **2,** 26, 2006.
7. Jain, R.K., Au, P., Tam, J., Duda, D.G., and Fukumura, D. Engineering vascularized tissue. Nat Biotechnol **23,** 821, 2005.
8. Ko, H.C., Milthorpe, B.K., and McFarland, C.D. Engineering thick tissues—the vascularisation problem. Eur Cells Mater **14,** 1; discussion 9, 2007.
9. Chang, C.C., and Hoying, J.B. Directed three-dimensional growth of microvascular cells and isolated microvessel fragments. Cell Transplant **15,** 533, 2006.
10. Salzmann, D.L., Kleinert, L.B., Berman, S.S., and Williams, S.K. Inflammation and neovascularization associated with clinically used vascular prosthetic materials. Cardiovasc Pathol **8,** 63, 1999.
11. Krishnan, L., Underwood, C.J., Maas, S., Ellis, B.J., Kode, T.C., Hoying, J.B., and Weiss, J.A. Effect of mechanical boundary conditions on orientation of angiogenic microvessels. Cardiovasc Res **78,** 324, 2008.
12. Zilberberg, L., Shinkaruk, S., Lequin, O., Rousseau, B., Hagedorn, M., Costa, F., Caronzolo, D., Balke, M., Canron, X., Convert, O., Lain, G., Gionnet, K., Goncalves, M., Bayle, M., Bello, L., Chassaing, G., Deleris, G., and Bikfalvi, A. Structure and inhibitory effects on angiogenesis and tumor development of a new vascular endothelial growth inhibitor. J Biol Chem **278,** 35564, 2003.
13. Ramsey, F.L., and Schafer, D.W. The Statistical Sleuth: A Course in Methods of Data Analysis, 2nd edition. Australia; Pacific Grove, CA: Duxbury/Thomson Learning, 2002.
14. Yamakawa, M., Liu, L.X., Date, T., Belanger, A.J., Vincent, K.A., Akita, G.Y., Kuriyama, T., Cheng, S.H., Gregory, R.J., and Jiang, C. Hypoxia-inducible factor-1 mediates activation of cultured vascular endothelial cells by inducing multiple angiogenic factors. Circ Res **93,** 664, 2003.
15. Jensen, R.L., Ragel, B.T., Whang, K., and Gillespie, D. Inhibition of hypoxia inducible factor-1alpha (HIF-1alpha) decreases vascular endothelial growth factor (VEGF) secretion and tumor growth in malignant gliomas. J Neurooncol **78,** 233, 2006.
16. Yancopoulos, G.D., Davis, S., Gale, N.W., Rudge, J.S., Wiegand, S.J., and Holash, J. Vascular-specific growth factors and blood vessel formation. Nature **407,** 242, 2000.
17. Ferrara, N., Chen, H., Davis-Smyth, T., Gerber, H.P., Nguyen, T.N., Peers, D., Chisholm, V., Hillan, K.J., and Schwall, R.H. Vascular endothelial growth factor is essential for corpus luteum angiogenesis. Nat Med **4,** 336, 1998.
18. Krishnan, L., Hoying, J.B., Nguyen, H., Song, H., and Weiss, J.A. Interaction of angiogenic microvessels with the extracellular matrix. Am J Physiol Heart Circ Physiol **293,** H3650, 2007.
19. Bishop, A. Role of oxygen in wound healing. J Wound Care **17,** 399, 2008.
20. Jain, R.K. Molecular regulation of vessel maturation. Nature Med **9,** 685, 2003.
21. Pepper, M.S. Manipulating angiogenesis. From basic science to the bedside. Arterioscler Thromb Vasc Biol **17,** 605, 1997.

Address correspondence to:
James B. Hoying, Ph.D.
Division of Cardiovascular Therapeutics
Cardiovascular Innovation Institute
Room 511, 302 E. Muhammad Ali Blvd.
Louisville, KY 40202

E-mail: jay.hoying@louisville.edu

Received: June 3, 2009
Accepted: September 23, 2009
Online Publication Date: December 18, 2009